

Effect of the concentration of the substitution impurity strontium on the magnetic ordering temperature in $\text{La}_{1-x}\text{Sr}_x\text{FeO}_{3-\delta}$ and its sensitivity to heat treatment

© A.I. Dmitriev, M.S. Dmitrieva

Federal Research Center for Problems of Chemical Physics and Medical Chemistry, Russian Academy of Sciences, Chernogolovka, Moscow region, Russia
E-mail: aid@icp.ac.ru

Received December 20, 2024

Revised January 22, 2025

Accepted January 22, 2025

Using simple quantitative methods based on the concepts of exchange field, Dzyaloshinskii field and magnetic anisotropy field, the effect of lanthanum substitution by strontium on the main macro- and microscopic magnetic characteristics of $\text{La}_{1-x}\text{Sr}_x\text{FeO}_{3-\delta}$ was assessed

Keywords: Substituted lanthanum orthoferrites, canted antiferromagnetism, vacuum annealing.

DOI: 10.61011/0000000000

Rare-earth orthoferrites with general formula $R\text{FeO}_3$ (R is a rare-earth ion) have attracted increased research attention for several decades due to their weak ferromagnetism, remarkable magnetooptical properties, spin-reorientation transitions, high velocities of domain wall motion, and various other properties [1]. At present, their physical properties still remain in the focus of attention of a considerable number of research groups, since they have high potential for application in innovative spintronics devices. In addition, they have contributed to the emergence of a new class of materials: multiferroics with strong magnetoelectric coupling [1]. Rare-earth $R\text{FeO}_3$ orthoferrites have a distorted perovskite structure with just one type of sites of Fe^{3+} ions coordinated octahedrally by six O^- ions. Their complex non-collinear magnetic structures and magnetic phase transitions are shaped primarily by the combination of a strong isotropic superexchange interaction with an antisymmetric Dzyaloshinskii–Moriya exchange interaction [1]. Data on the structure–property relations are needed both to clarify the nature of physical properties of novel materials and to accelerate their introduction into practice. Perovskites with octahedral rotations and distortions have already been examined by group-theoretical methods [2]. The relation between the rotation angles of octahedra and the binding energy in crystals with a perovskite structure was examined in [3]. Despite impressive advances in modern *ab initio* methods of band structure calculation and various quantum-chemical calculation methods, they provide only a very rough description of the electronic structure and energy spectrum, which may serve only as a proposal for experiments, of most systems of practical importance. There are virtually no examples of successful application of experimental structure–property relations in quantitative analysis of fine exchange effects and magnetic anisotropy effects in perovskites (in particular, orthoferrites). The aim of the present study is to establish the influence

of substitutional strontium on the magnetic anisotropy and hysteresis in $\text{La}_{1-x}\text{Sr}_x\text{FeO}_{3-\delta}$.

Polycrystalline $\text{La}_{1-x}\text{Sr}_x\text{FeO}_{3-\delta}$ ($x = 0.33, 0.50, 0.67$) samples were synthesized by the sol-gel method with the use of Sr, Fe, and La nitrates in a stoichiometric ratio as initial reagents. These samples are denoted as Sr33, Sr50, and Sr67. The specifics of sample preparation and their composition and structure were detailed in [4–6]. Dependences $M(H)$ of magnetization on magnetic field strength were measured with a vibration magnetometer of the multifunctional cryogen free measurement system (CFMS) from Cryogenic Ltd, U.K.

Temperature dependences of magnetization $M(T)$ of samples Sr33, Sr50, and Sr67 have been examined in detail in our recent studies [7,8]. Néel temperature T_N at which weak ferromagnetism is established was determined for each of them. The introduction of a substitutional impurity (strontium) into $\text{La}_{1-x}\text{Sr}_x\text{FeO}_{3-\delta}$ and an increase in its concentration lead to a significant reduction of the magnetic ordering temperature (Fig. 1). The observed effects of Néel temperature variation were attributed in [7,8] to a change in the valence state of iron ions and the Fe–O–Fe bond angles and to the emergence of oxygen vacancies during substitution. Since the electrical neutrality of $\text{La}_{1-x}\text{Sr}_x\text{FeO}_{3-\delta}$ needs to be maintained, the substitution of La^{3+} ions with Sr^{2+} ions causes the transformation of a certain fraction of Fe^{3+} into Fe^{4+} and the production of oxygen vacancies [4–6].

According to the Goodenough’s theory, the superexchange interaction between Fe^{3+} and Fe^{3+} ions is antiferromagnetic and stronger than the one between Fe^{4+} and Fe^{4+} ions or Fe^{3+} and Fe^{4+} [9]. Moreover, according to Zener’s theory, the latter ions have a ferromagnetic channel between them established via double exchange [10–14]. Emerging oxygen vacancies disrupt the exchange coupling. Therefore, the introduction of Sr^{2+} ions into lanthanum orthoferrite, on

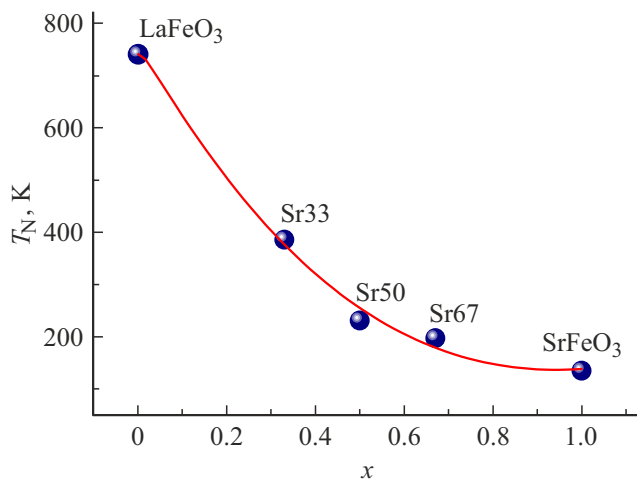


Figure 1. Dependence of Néel temperature T_N on the amount of strontium dopant (x). The solid curve is the approximating one.

the one hand, weakens the antiferromagnetic superexchange interaction (J_{AF}) and, on the other hand, induces the ferromagnetic double exchange interaction (J_F). Resulting exchange integral J_{ex} is an additive physical quantity that is a linear combination of J_{AF} and J_F . It is impossible to separate quantitatively the contributions of J_{AF} and J_F into J_{ex} . Weakening of J_{AF} with simultaneous intensification of J_F leads to weakening of J_{ex} and a reduction in Néel temperature T_N [15] (Fig. 1). Therefore, only J_{ex} may be estimated quantitatively based on the known relation between J_{ex} and T_N : $T_N = zS(S+1)J_{ex}/3k_B$, where $z = 6$ is the number of nearest neighbors, $S = 5/2$ is the spin of iron Fe^{3+} ions, and k_B is the Boltzmann constant [1]. First, if T_N is known, this expression allows one estimate directly the values of exchange integrals J_{ex} for each of the three samples (see the table). Second, it provides a simple explanation for the $T_N(x)$ dependence, attributing it to dependence $J_{ex}(x)$. Changes in the crystal structure of $La_{1-x}Sr_xFeO_{3-\delta}$ occurring when La^{3+} is substituted with Sr^{2+} always lead, among other things, to a reduction of Fe–O–Fe bond angle θ . It decreases with increasing x in a power-law fashion: $\theta(x) = a - bx^c$ [16]. The superexchange interaction intensifies with increasing Fe–O–Fe bond angle θ as $J_{ex}(\theta) = A + B \cos \theta + C \cos^2 \theta$ [1]. It follows from this expression that superexchange integral J_{ex} reaches its maximum at $\theta = 180^\circ$. Thus, the $J_{ex}(x)$ dependence is a mediated $\theta(x)$ dependence. The solid

curve in Fig. 1 represents an approximation of the $T_N(x)$ dependence through the $J_{ex}(\theta)$ dependence with empirical relation $\theta(x)$ taken into account. The approximation parameters were as follows: $a = 180^\circ$, $b = 80^\circ$, $c = 0.5$, $A = 10$ K, $B = 35$ K, and $C = 60$ K; i.e., the reduction of J_{ex} with increasing x (see the table) is attributed to the fact that the bond angle decreases from $\theta = 140$ to 125° as x grows from 0.33 to 0.67. To conclude this section, we note that the values of exchange field $H_{ex} = zSJ_{ex}/g\mu_B$ were determined for each of the three samples (see the table). In the given expression, $g = 2$ is the g -factor of Fe^{3+} ions and μ_B is the Bohr magneton. The value of exchange field H_{ex} is important not in itself, but for further discussion. The exchange field values estimated this way are marked with subscript 1 in the table (H_{ex1}). Figure 2 shows dependences $M(H)$ of magnetization on magnetic field strength at a temperature of 2 K for samples Sr33, Sr50, and Sr67. The shape of the $M(H)$ curves is typical of weak ferromagnets. One remarkable feature stands out. The magnetization decreases with an increase in x in relatively weak magnetic fields $H < 10$ kOe, while the pattern in strong fields with $H > 10$ kOe is reversed: the magnetization increases with x (Fig. 2). In weak magnetic fields, when the orienting effect of the external magnetic field is imperceptible, we are dealing with the magnetization of a weak ferromagnet in the basal plane, which depends on H as $M(H) = \chi H_D + \chi H$ [17–19]. This expression was used to approximate the experimental $M(H)$ dependences (purple curves in Fig. 2). Here, χ is the magnetic susceptibility and H_D is the Dzyaloshinskii field. The values of χ and H_D were determined directly from the approximation, while spontaneous magnetization σ and exchange field H_{ex} were determined using relations $\sigma = \chi H_D$ and $\chi = M_{Fe}/2H_{ex}$ (see the table) [19]. Here, $M_{Fe} = 2gS\mu_B/\rho V \approx 60$ emu/g is the magnetization of one of the sublattices of the antiferromagnet (see the table) [1]. The exchange field values estimated this way are marked with subscript 2 in the table (H_{ex2}). The values of H_{ex1} and H_{ex2} obtained as a result of analysis of completely different dependences $T_N(x)$ and $M(H)$ are very close and decrease with increasing x (see the table). However, the main result here is that a reduction in σ with an increase in x follows from the above estimates. Thus, the measured magnetization in weak magnetic fields $H < 10$ kOe decreases with increasing x due to the fact that σ decreases with increasing x . The spontaneous magnetization of a weak ferromagnet depends on the ratio of contributions

Magnetic characteristics of samples

x	T_N , K	J_{ex} , K	H_{ex1} , T	H_D , T	χ , emu/(g·T)	σ emu/g	H_{ex2} , T	$H_D/2H_{ex}$	M_s , emu/g	H_a , T	K , 10^4 erg/cm ³	H_c , T	M_r , emu/g
0.33	385	32	246	2.3	0.12	0.27	247	0.005	0.9	2.3	6.6	0.99	0.24
0.50	230	19	147	0.7	0.23	0.16	130	0.003	0.5	2.1	3.5	0.37	0.15
0.67	196	16	125	0.5	0.26	0.14	126	0.002	0.4	1.3	1.6	0.06	0.07

of the isotropic superexchange interaction (H_{ex}) and the antisymmetric Dzyaloshinskii–Moriya exchange interaction (H_D) to the total effective exchange and is written as $\sigma = M_{Fe}H_D/2H_{ex}$ [19]. Factor $H_D/2H_{ex}$ characterizes the canting angle of the antiferromagnet sublattices, which, in accordance with expression $\sin \varphi = (H_D + H)/2H_{ex}$, decreases from $\varphi = 0.5$ to 0.2° as x increases from 0.33 to 0.67 [19]. It can be seen from the table that both H_D and H_{ex} decrease with increasing x , but their contributions are redistributed in such a way that σ decreases as x grows. While the first contribution depends primarily on the Fe–O–Fe bond angle, the second one depends both on the superexchange bond angle and on its spatial orientation. To conclude, we note that the estimated σ values for all three samples are close to remanent magnetization M_r (see the table). As was already noted, the magnetization increases with an increase in x in strong magnetic fields $H > 10$ kOe (see the table). In magnetic fields stronger than a certain level (magnetic anisotropy field H_a), the orienting effect of the external magnetic field becomes significant. In fields $H > H_a$, a weak ferromagnet also acquires an orthogonal magnetization component, which is inversely proportional to H_a . Therefore, the increasing dependence of magnetization $M(x)$ recorded in high magnetic fields may be attributed qualitatively to decreasing dependence $H_a(x)$. In the region of strong magnetic fields, when the magnetization approaches saturation M_s , it has a power-law dependence on H : $M(H) = M_s(1 - (H_a/H)^2) + \chi H$ [20]. This expression was used to approximate high-field ($H > 40$ kOe) experimental dependences $M(H)$ with extrapolation of magnetization to $H = 0$ Oe for visualization of field H_a (red curves in Fig. 2). It can be seen from the table that the values of both M_s and H_a determined directly from the approximation decrease with increasing x . The value of magnetization M_s determined from the approximation and the theoretical value of $M_s = 2M_{Fe}H_D/H_{ex}$ agree closely with each other [19]. The behavior of $M(x)$ was discussed in detail above. The key feature of interest to us here is that the introduction of substitutional strontium into $La_{1-x}Sr_xFeO_{3-\delta}$ and an increase in its concentration lead to noticeable weakening of magnetic anisotropy H_a . The H_a anisotropy field is the limiting value of coercive force H_c . Therefore, both coercive force H_c and the H_a anisotropy field are expected to decrease with increasing x . The magnetic hysteresis loops (Fig. 3) were measured to verify this assumption. The parameters of these loops (coercive force H_c and remanent magnetization M_r) are given in the table. We have already noted that the values of remanent magnetization M_r for all three samples turned out to be close to the values of spontaneous magnetization σ . As expected, coercive force H_c decreases, in synchrony with H_a , with increasing x . This indicates that the $H_c(x)$ dependence is shaped by variations of magnetic anisotropy with increasing x rather than by changes in the microstructure of samples. The value of magnetic anisotropy constant K was estimated for each of the three samples using the known $H_a = 2K/M_s$ relation. It turned out that

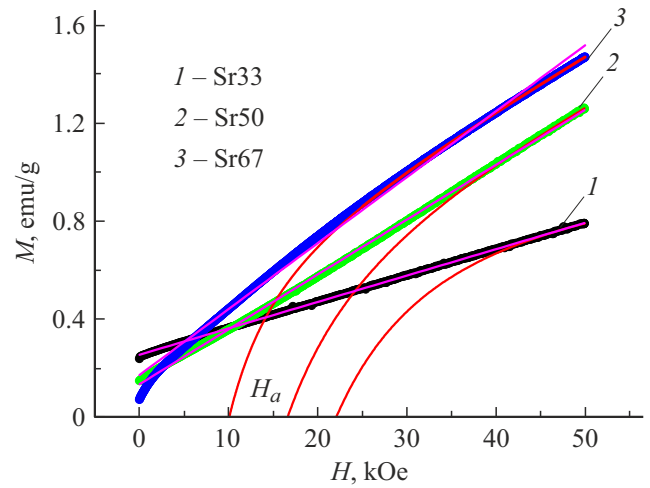


Figure 2. Dependences of magnetization of samples Sr33 (black symbols), Sr50 (green symbols), and Sr67 (blue symbols) on magnetic field strength at a temperature of 2 K. Solid purple and red curves are the approximating ones. A color version of the figure is provided in the online version of the paper.

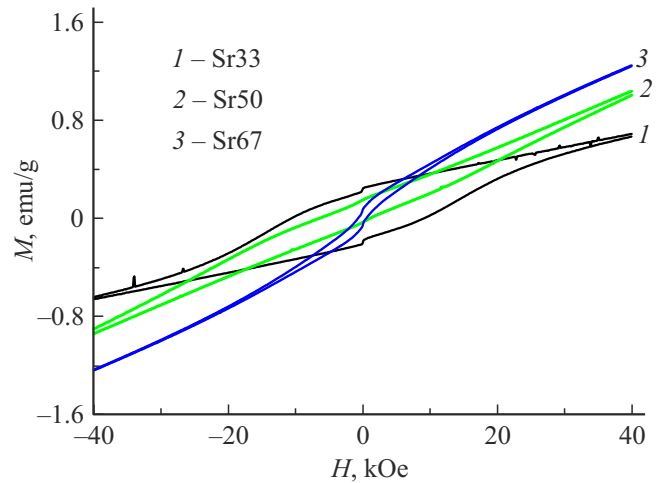


Figure 3. Magnetic hysteresis loops of samples Sr33, Sr50, and Sr67 at a temperature of 2 K.

it decreases with increasing x (see the table) [20]. If one tracks the variations of both magnetic anisotropy constant K and Dzyaloshinskii field H_D with increasing x in the table, it becomes evident that K increases with H_D . In other words, as the antisymmetric Dzyaloshinskii–Moriya exchange interaction grows stronger, the magnetic anisotropy increases. This may imply that the spin-orbit interaction is the main microscopic mechanism behind these two phenomena. The Dzyaloshinskii–Moriya interaction induces the formation of a non-collinear antiferromagnetic spin structure with a loosely antiparallel arrangement of spins of iron ions in the samples.

Thus, the dependences of the Néel temperature on the amount of strontium dopant ($T_N(x)$) and the magnetization on the magnetic field strength ($M(x, H)$) at a temperature

of 2 K were analyzed thoroughly for a series of three $\text{La}_{1-x}\text{Sr}_x\text{FeO}_{3-\delta}$ ($x = 0.33, 0.50, 0.67$) samples. It was established that temperature T_N decreases with an increase in x due to weakening of the superexchange interaction caused by a reduction of the Fe–O–Fe bond angle with increasing x . The variations of $M(x, H)$ in weak magnetic fields are attributable to the redistribution of contributions of the isotropic superexchange interaction and the antisymmetric Dzyaloshinskii–Moriya exchange interaction to the total effective exchange; in high fields, they are induced by magnetic anisotropy effects. It was demonstrated that the decreasing dependence of coercive force $H_c(x)$ is formed by variations of magnetic anisotropy rather than by changes in the microstructure of samples. The spin-orbit interaction is the main microscopic mechanism that shapes magnetic anisotropy.

Funding

This study was supported by the Ministry of Science and Higher Education of the Russian Federation under state assignment No. 124013100858-3.

Conflict of interest

The authors declare that they have no conflict of interest.

References

- [1] A. Moskvina, *Magnetochemistry*, **7** (8), 111 (2021). DOI: 10.3390/magnetochemistry7080111
- [2] P.V. Balachandran, J.M. Rondinelli, *Phys. Rev. B*, **88** (5), 054101 (2013). DOI: 10.1103/PhysRevB.88.054101
- [3] N.M. Olekhovich, *Crystallogr. Rep.*, **52** (5), 759 (2007). DOI: 10.1134/S106377450705001X
- [4] V.D. Sedykh, O.G. Rybchenko, N.V. Barkovskii, A.I. Ivanov, V.I. Kulakov, *Phys. Solid State*, **63** (12), 1775 (2021). DOI: 10.1134/S1063783421100322
- [5] V. Sedykh, O. Rybchenko, V. Rusakov, S. Zaitsev, O. Barkalov, E. Postnova, T. Gubaidulina, D. Pchelina, V. Kulakov, *J. Phys. Chem. Solids*, **171**, 111001 (2022). DOI: 10.1016/j.jpcs.2022.111001
- [6] V. Sedykh, V. Rusakov, O. Rybchenko, A. Gapochka, K. Gavrilicheva, O. Barkalov, S. Zaitsev, V. Kulakov, *Ceram. Int.*, **49** (15), 25640 (2023). DOI: 10.1016/j.ceramint.2023.05.105
- [7] M.S. Dmitrieva, A.I. Dmitriev, V.D. Sedykh, *Bull. Russ. Acad. Sci. Phys.*, **88** (12), 2047 (2024). DOI: 10.1134/S10628738240708663
- [8] A.I. Dmitriev, S.V. Zaitsev, M.S. Dmitrieva, *Tech. Phys. Lett.*, **50** (7), 21 (2024). DOI: 10.61011/0000000000
- [9] J.B. Goodenough, *Magnetism and the chemical bond* (Wiley, N.Y., 1963).
- [10] P.S.J. Bharadwaj, S. Kundu, V.S. Kolipara, K.B.R. Varma, *RSC Adv.*, **10**, 22183 (2020). DOI: 10.1039/D0RA02532A
- [11] S. Erat, A. Braun, C. Piamonteze, Z. Liu, A. Ovalle, H. Schindler, T. Graule, L.J. Gauckler, *J. Appl. Phys.*, **108** (12), 124906 (2010). DOI: 10.1063/1.3517822
- [12] A.S. Kumar, S. Srinath, *AIP Adv.*, **4** (8), 087144 (2014). DOI: 10.1063/1.4894486
- [13] R.J. McQueeney, J. Ma, S. Chang, J.-Q. Yan, M. Hehlen, F. Trouw, *Phys. Rev. Lett.*, **98** (12), 126402 (2007). DOI: 10.1103/PhysRevLett.98.126402
- [14] F. Gao, P.L. Li, Y.Y. Weng, S. Dong, L.F. Wang, L.Y. Lv, K.F. Wang, J.-M. Liu, *Appl. Phys. Lett.*, **91** (7), 072504 (2007). DOI: 10.1063/1.2768895
- [15] Y.-Q. Liang, N.-L. Di, Z.-H. Cheng, *Phys. Rev. B*, **72** (13), 134416 (2005). DOI: 10.1103/PhysRevB.72.134416
- [16] L. Huang, L. Cheng, S. Pan, Y. He, C. Tian, J. Yu, H. Zhou, *Ceram. Int.*, **46** (17), 27352 (2020). DOI: 10.1016/j.ceramint.2020.07.220
- [17] J.B. Yang, W.B. Yelon, W.J. James, Z. Chu, M. Kornecki, Y.X. Xie, X.D. Zhou, H.U. Anderson, A.G. Joshi, S.K. Malik, *Phys. Rev. B*, **66** (18), 184415 (2002). DOI: 10.1103/PhysRevB.66.184415
- [18] A.S. Borovik-Romanov, V.I. Ozhogin, *Sov. Phys. JETP*, **12** (1), 18 (1961).
- [19] E.A. Turov, *Sov. Phys. JETP*, **9** (4), 890 (1959).
- [20] S. Leclashree, P.D. Babu, S.N. Kaul, S. Srinath, *J. Alloys Compd.*, **905**, 164145 (2022). DOI: 10.1016/j.jallcom.2022.164145

Translated by D.Safin